Assessing Compressive Strength of Reclaimed Clay Bricks Using SWIR Hyperspectral Imaging and Deep Learning

Jean-Philippe Andreu, Maria Jernej
JOANNEUM RESEARCH
Graz, Austria
{firstname.lastname}@joanneum.at

Maximilian Klammer, Benjamin Kromoser
Universität für Bodenkultur Wien
Vienna, Austria
{firstname.lastname}@boku.ac.at

Abstract

A non-destructive approach is proposed to assess the compressive strength of reclaimed bricks using short-wave infrared (SWIR) hyperspectral imaging (HSI) and a spectral–spatial 1D-Convolutional Neural Network (CNN). Hyperspectral images of 60 bricks, capturing both outer (weathered) and inner (pristine) surfaces, were analyzed. Regression reached $R^2 = 0.625$, while a three class (*low*, *medium*, *high*) compressive strength classification achieved $83\,\%$ pixel level accuracy. At the brick level, aggregating predictions with a majority-vote scheme attained an accuracy of $91\,\%$ for outer and $98\,\%$ for inner surfaces. Score-CAM identified key wavelengths around 1200–1400 nm (moisture) and 2300–2500 nm (clay minerals) as driving the predictions. The results demonstrate that SWIR HSI can capture mineral- and moisture-related signatures relevant to compressive strength, offering a rapid, non-destructive screening tool for reclaimed bricks.

1 Introduction

Construction and demolition waste accounts for over a third of total waste in the European Union, highlighting the need for effective material recovery strategies. Within the circular economy framework, the European Commission promotes approaches that retain material value while minimizing additional processing. Clay bricks are particularly suitable for reuse, as their material value is preserved and energy-intensive reprocessing avoided [2]. Before reuse, however, material performance must be verified by assessing properties such as compressive strength, frost resistance, and water absorption [10]. Standard compressive strength testing involves crushing representative bricks in a hydraulic press, with the average strength determining the strength class. As this method is destructive and time-consuming, it is unsuitable for rapid screening of large quantities of reclaimed bricks.

Therefore, non-destructive techniques that enable rapid assessment of brick quality are of increasing interest. One promising approach is SWIR HSI, which provides information about both mineral composition and moisture content. Clay bricks are primarily composed of clay minerals such as kaolinite and montmorillonite, along with silicate minerals. These clay minerals exhibit characteristic absorption features in the SWIR region, particularly between $2000\,\mathrm{nm}$ and $2500\,\mathrm{nm}$ due to vibrational overtones and combination bands of hydroxyl (OH), metal–OH, and H_2O molecular bonds [13]. These spectral features allow the mineral composition to be inferred from hyperspectral data, which is closely linked to firing behavior, porosity, microstructure, and thus indirectly to compressive strength. SWIR wavelengths are also highly sensitive to water, with strong absorption bands near $1400\,\mathrm{nm}$ and $1900\,\mathrm{nm}$ [7, 9]. In porous ceramic materials such as bricks, moisture uptake is largely governed by open porosity, which in turn is again closely related to compressive strength [4]. Relationships between SWIR spectral features and compressive strength have been reported for several geomaterials. SWIR absorption bands related to clay minerals and alteration phases show negative correlations

The Third Austrian Symposium on AI, Robotics, and Vision (AIROV26).

with compressive strength of granite [12]. Similar correlations have also been observed in soils [8], carbonates [1], volcanic rocks [6] and water-bearing sandstones [14].

In this work, a spectral–spatial 1D-CNN framework, initially introduced by Hsieh and Kiang [5] on remote sensing hyperspectral data, was applied in a regression setting to investigate whether compressive strength can be predicted directly from SWIR hyperspectral images of demolition bricks. The model was subsequently repurposed for a three-class classification task, reflecting common practice in the construction industry where bricks are typically evaluated against compressive strength thresholds. In addition, post-hoc explainability using Score-CAM was applied to identify the wavelengths most relevant to the model's predictions.

2 Data Collection

A total of sixty bricks were extracted from different walls of a more than 100 years old building scheduled for demolition in Vienna, Austria. Buildings of this age typically contain bricks from different production batches and factories, as indicated by the different manufacturer stamps found on the samples. However, as all bricks originate from a single building, including samples from multiple demolition sites would further increase dataset diversity and should be considered in future work.

After extraction, the bricks were split in half immediately. One half of each brick was sealed to preserve its original moisture content, and the other half was stored to dry. Only the dried halves were used in the present experiments to reduce variability. In practical applications, bricks would likely be analyzed immediately after extraction. Therefore, the influence of site-specific moisture needs to be investigated in the future. Two surfaces of each selected half were imaged: (i) the largest outer face, which may contain dust, mortar residues, or other surface coatings, and (ii) the freshly exposed inner surface created by splitting the brick, representing uncontaminated brick material.

All images were acquired using a Specim SWIR hyperspectral push-broom camera, covering the spectral range of $1000\,\mathrm{nm}$ to $2500\,\mathrm{nm}$ with a spectral resolution of $12\,\mathrm{nm}$ for a total of 288 bands. A two-sided halogen lamp illumination was supplemented by a quartz glass rod to extend the spectral coverage toward the thermal range. The data were radiometrically calibrated to obtain relative reflectance, eliminating the influence of illumination and sensor response. Dark and white references were recorded using a black cold cloth and a Spectralon target, and each pixel spectrum was normalized against these references. After data acquisition, all bricks were subjected to an irreversible uniaxial compressive strength test at the University of Natural Resources and Life Sciences Vienna (BOKU). The resulting compressive strength values (in MPa) serve as ground-truth measurements.

3 Methodology

Instead of using transfer learning with an established backbone like ResNet [3] (which would require an early frequency selection / dimensional reduction in order to fit the required 3 input channels) we opted to follow Hsieh and Kiang [5], exploiting a 1D-CNN with spectral-spatial input features (rather than single spectra) to take into account the heterogeneous brick surfaces. For each target pixel, a 3×3 neighborhood was extracted and the nine spectral signatures were stacked together, yielding an input tensor of dimension $9 \times F$ (with $F = 288$ SWIR spectral bands). This representation encodes local texture and reduces sensitivity to single-pixel noise, relevant for heterogeneous brick surfaces.

A 1D-CNN regression model was designed with the following sequential architecture:

- 1D Convolutional layer: 40 filters of size 5×1, applied across the spectral dimension
- 1D Max pooling layer: factor-of-2 down-sampling followed by a ReLU activation function
- 1D Convolutional layer: 80 filters of size 5×1
- 1D Max pooling layer: factor-of-5 down-sampling followed by a ReLU activation function
- Intermediate fully connected linear layer with output size of 100
- Output fully connected linear layer for scalar regression (compressive strength in MPa)

Batch normalization was used after each convolutional layer to stabilize the learning process.

For classification, the same convolutional backbone was retained and a softmax function applied to the output of the final layer in order to get the probability distribution over the three compressive strength classes (*low*, *medium* and *high*). For this experiment, the boundaries of the three compressive

strength classes were automatically selected as the 1/3 and 2/3 percentiles of the compressive strength values of the dataset: $< 9.95\,\mathrm{MPa}$ (*low*), $9.95\,\mathrm{MPa}$ – $13\,\mathrm{MPa}$ (*medium*) and $> 13\,\mathrm{MPa}$ (*high*).

The network was implemented in PyTorch and trained using the Adam optimizer with a learning rate of 10^{-3} and a mean-squared-error loss for regression (cross-entropy for classification). The training was run over 2000 epochs with a confidence-based early exit strategy.

For each brick sample, 2000 spectral-spatial patches were extracted at random, resulting in a 120,000 sample dataset. It was then partitioned into $60\,\%$ training, $20\,\%$ validation and $20\,\%$ test sets using stratified sampling to balance the representation of outer and inner surfaces and strength ranges across splits.

4 Results

The performance of the regression model on the test set yielded the following results: a RMSE of $2.35\,\mathrm{MPa}$, a MAE of $1.76\,\mathrm{MPa}$ and a R^2 of 0.625 (Fig. 1a). Approximately $63\,\%$ of the variance in compressive strength is explained by the model spectral-spatial input alone. The MAE of $1.76\,\mathrm{MPa}$ is operationally meaningful given typical quality-class boundaries of $5\,\mathrm{MPa}$ to $10\,\mathrm{MPa}$ in brick standards.

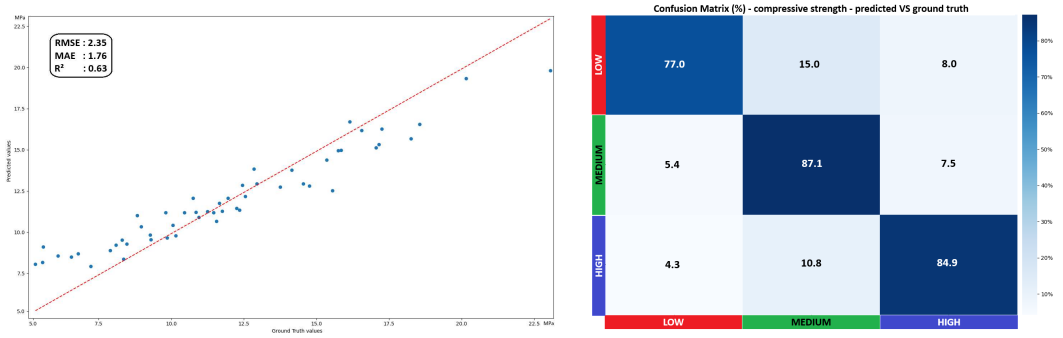

(a) Regression - Correlation Plot

(b) Classification - Confusion Matrix

Figure 1: Regression and classification results for the compressive strength of the reclaimed bricks.

When the CNN backbone was applied as a three-class classifier (*low*, *medium* and *high* compressive strength), pixel-level predictions on the test set achieved an overall accuracy of $83\,\%$ (Fig. 1b). Misclassifications were primarily caused by surface contamination (dust, coatings or weathering crusts) and small-scale material variability, rather than systematic differences between class boundaries. A comparison between the rendered (with false colors from the HSI data) image of a sample outer-face (Fig. 2a) and its pixelwise classification (Fig. 2b) shows the influence on the classification of localized surface contamination. We noticed that inner surfaces, due to their cleaner and more homogeneous composition, generally produced lower prediction variance on classification results. To estimate the overall strength of each brick in a way that reflects conventional compressive testing, a majority-vote scheme was applied across all pixels. At the brick-level we reached an accuracy of $91\,\%$ for the outer-face classification and $98\,\%$ for the inner-surface classification. This aggregation improved brick-level classification accuracy, and for the few bricks that remained misclassified after majority voting, errors were mostly concentrated at the boundaries between adjacent classes, consistent with the continuous and overlapping nature of compressive-strength distributions.

To gain insight into the spectral regions driving the three-class classifier, Score-CAM [11] was applied as a post-hoc explainability tool. Score-CAM generates gradient-free saliency maps by weighting each activation map according to its forward-passing score on the target class, thus identifying which part of the input data (i.e. spectral channels) contribute most to a given prediction. A strong influence of the spectral regions ranging from $1200\,\mathrm{nm}$ to $1400\,\mathrm{nm}$ and from $2300\,\mathrm{nm}$ to $2500\,\mathrm{nm}$ was observed for all compressive strength classes (high confidence on the jet color scale of Fig. 3). Still, the contribution of that last range was more pronounced in the *high* compressive strength class. Furthermore, we identified an influence of the wavelengths around $1900\,\mathrm{nm}$ on the predictions for the *medium* class (Fig. 3). These findings can be physically interpreted: the regions around $1400\,\mathrm{nm}$ and $1900\,\mathrm{nm}$ correspond to known water absorption bands, where elevated moisture content, indicative

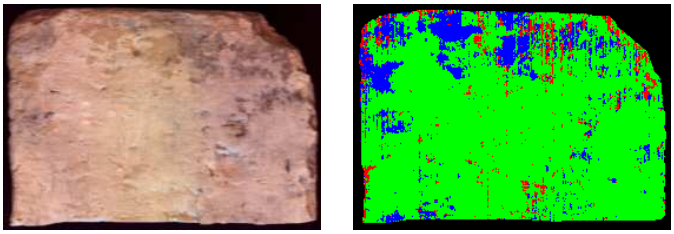

(a) Rendered RGB (false colors) (b) Classification

Figure 2: Pixelwise classification (low | medium | high compressive strength) of a outer face sample with a measured (destructively) high compressive strength value of 11.6 MPa

of higher open porosity, is associated with weaker bricks [7]. The prominence of the 2300 nm to 2500 nm range corresponds to the characteristic absorption features of clay minerals [13, 12], the abundance of which indicates the composition of the brick. Together, these results confirm that the CNN has learned physically meaningful features rather than spurious correlations.

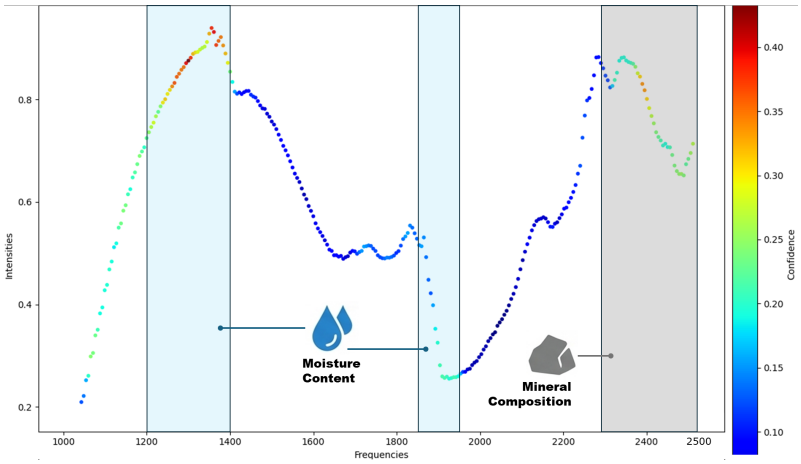

Figure 3: Average Score-CAM results for 100 spectra of the *medium* compressive strength class.

5 Conclusion and Outlook

We have demonstrated that SWIR HSI can capture mineralogical and moisture-related features and, combined with a spectral-spatial 1D-CNN, it enables the estimation of compressive strength in reclaimed bricks (regression: MAE 1.76 MPa, $R^2 = 0.625$). For classification into three compressive strength classes, a pixel-level accuracy of 83 % was reached, increasing to 91 % (outer) and 98 % (inner) at the brick level when using majority voting.

Compressive strength measurements provide a single bulk value for each brick. For this reason, majority voting was used to aggregate pixel-level predictions into a brick-level estimate that is comparable to the measured value. However, the measured compressive strength is also influenced by local instabilities, inclusions, and cracks. Such structural information is lost when reducing spatially resolved predictions to a single value through majority voting. Future work should therefore investigate how structural effects influence the overall compressive strength and develop more advanced classification schemes that integrate pixel-wise predictions into a structural assessment of the brick, providing an overall strength score. In addition, HSI is a surface inspection method and cannot detect structural defects located inside the brick. It therefore remains unclear whether surface information alone is sufficient to reliably predict compressive strength or whether complementary bulk measurements are required. This should be further investigated using techniques such as X-ray or CT imaging and acoustic testing to capture internal structural features.

Acknowledgments and Disclosure of Funding

The present work was funded by the Austrian Research Promotion Agency (FFG) through project KRAISBAU (48302986). The authors would furthermore like to thank University of Natural Resources and Life Sciences Vienna (BOKU) for extracting the brick samples and for carrying out the compressive strength measurements.

References

[1] D. Bakun-Mazor, Y. Ben-Ari, G. Notesko, S. Marco, and E. Ben-Dor. Measuring carbonate rock strength using spectroscopy across the optical and thermal region. *IOP Conference Series: Earth and Environmental Science*, 833(1):012025, August 2021.

[2] J. Cristobal Garcia, D. Caro, G. Foster, G. Pristera, F. Gallo, and D. Tonini. Techno-economic and environmental assessment of construction and demolition waste management in the European Union, 2024.

[3] K. He, X. Zhang, S. Ren, and J. Sun. Deep residual learning for image recognition. In *Proceedings of the IEEE conference on computer vision and pattern recognition*, pages 770–778, 2016.

[4] M. He, Z. Zhang, J. Zhu, and N. Li. Correlation between the constant m_i of Hoek–Brown criterion and porosity of intact rock. *Rock Mechanics and Rock Engineering*, 55(2):923–936, February 2022.

[5] T.-H. Hsieh and J.-F. Kiang. Comparison of CNN algorithms on hyperspectral image classification in agricultural lands. *Sensors*, 20(6):1734, March 2020.

[6] G. Kereszturi, M. Heap, L. N. Schaefer, H. Darmawan, F. M. Deegan, B. Kennedy, J.-C. Komorowski, S. Mead, M. Rosas-Carbajal, A. Ryan, V. R. Troll, M. Villeneuve, and T. R. Walter. Porosity, strength, and alteration – Towards a new volcano stability assessment tool using VNIR-SWIR reflectance spectroscopy. *Earth and Planetary Science Letters*, 602:117929, January 2023.

[7] B. Koirala and P. Scheunders. An efficient method for water content estimation of building materials from spectral reflectance. *NDT and E International*, 147:103214, October 2024.

[8] F. Mousavi, E. Abdi, P. Fatehi, A. Ghalandarzadeh, H. A. Bahrami, B. Majnounian, and N. Ziadi. Rapid determination of soil unconfined compressive strength using reflectance spectroscopy. *Bulletin of Engineering Geology and the Environment*, 80(5):3923–3938, March 2021.

[9] M. Sadeghi, S. B. Jones, and W. D. Philpot. A linear physically-based model for remote sensing of soil moisture using short wave infrared bands. *Remote Sensing of Environment*, 164:66–76, July 2015.

[10] P. Stępień, E. Spychał, and K. Skowera. A comparative study on hygric properties and compressive strength of ceramic bricks. *Materials*, 15(21):7820, November 2022.

[11] H. Wang, Z. Wang, M. Du, F. Yang, Z. Zhang, S. Ding, P. Mardziel, and X. Hu. Score-CAM: score-weighted visual explanations for convolutional neural networks. In *2020 IEEE/CVF Conference on Computer Vision and Pattern Recognition Workshops (CVPRW)*, pages 111–119, 2020.

[12] E. C. Wellman, D. Riley, A. Hughes, N. Risso, M. Momayez, and J. Kemeny. A proposed concept for classifying uniaxial compressive strength (UCS) from SWIR hyperspectral data. *Engineering Geology*, 356:108300, September 2025.

[13] F. A. Yitagesu, F. van der Meer, H. van der Werff, and W. Zigterman. Quantifying engineering parameters of expansive soils from their reflectance spectra. *Engineering Geology*, 105(3–4):151–160, May 2009.

[14] X.-L. Zhang, F. Zhang, Y.-Z. Wang, Z.-G. Tao, and X.-Y. Zhang. Strength prediction model for water-bearing sandstone based on near-infrared spectroscopy. *Journal of Mountain Science*, 20(8):2388–2404, August 2023.